Natural Resources Canada
Ressources naturelles Canada

U, Th, and REE occurrences within Nueltin granite at Nueltin Lake, Nunavut: recent observations

J.M.J. Scott, T.D. Peterson, and M.W. McCurdy

Geological Survey of Canada
Current Research 2012-1

2012

Canada

Geological Survey of Canada
Current Research 2012-1

U, Th, and REE occurrences within Nueltin granite at Nueltin Lake, Nunavut: recent observations

J.M.J. Scott, T.D. Peterson, and M.W. McCurdy

2012

ISSN 1701-4387
Catalogue No. M44-2012/1E-PDF
ISBN 978-1-100-19548-3
doi: 10.4095/289393

A copy of this publication is also available for reference in depository libraries across Canada through access to the Depository Services Program's Web site at http://dsp-psd.pwgsc.gc.ca

A free digital download of this publication is available from GeoPub: http://geopub.nrcan.gc.ca/index_e.php

Toll-free (Canada and U.S.A.): 1-888-252-4301

Recommended citation

Scott, J.M.J., Peterson, T.D., and McCurdy, M.W., 2012. U, Th, and REE occurrences within Nueltin granite at Nueltin Lake, Nunavut: recent observations; Geological Survey of Canada, Current Research 2012-1, 11 p. doi: 10.4095/289393

Critical review
B. Kjarsgaard

Authors
J.M.J. Scott (justtrickin@hotmail.com)
Present address: Department of Earth Sciences
Carleton University
Ottawa, Ontario
K1S 5B6

J.M.J. Scott (justtrickin@hotmail.com)
T.D. Peterson (Tony.Peterson@NRCcan-RNCan.gc.ca)
M.W. McCurdy (Martin.McCurdy@NRCan-RNCan.gc.ca)
Geological Survey of Canada
601 Booth Street
Ottawa, Ontario
K1A 0E9

Correction date:

U, Th, and REE occurrences within Nueltin granite at Nueltin Lake, Nunavut: recent observations

J.M.J. Scott, T.D. Peterson, and M.W. McCurdy

Scott, J.M.J., Peterson, T.D., and McCurdy, M.W., 2012. U, Th, and REE occurrences within Nueltin granite at Nueltin Lake, Nunavut: recent observations; Geological Survey of Canada, Current Research 2012-1, 11 p. doi: 10.4095/289393

Abstract: Two anomalous occurrences of primary uranium, thorium, and rare-earth elements in the Nueltin Lake area are associated with an aplite dyke and a pegmatitic seam within the Nueltin granitic suite. The occurrences are rich in uranothorite and allanite, which are also present in the host Nueltin granite. The aplite dyke is enriched in uranium (56.8 ppm) and thorium (770 ppm), and the pegmatitic seam is enriched in uranium (610 ppm), thorium (8839 ppm) and rare-earth elements (total 86 153 ppm). These enrichments are 10 to 100 times that of the host pluton. Parallel-trending trace-element patterns indicate that the anomalies most likely represent late-stage, highly fractionated melts from the Nueltin granite.

Résumé : Dans la région du lac Nueltin, deux occurrences primaires anomales d'uranium, de thorium et de terres rares dans la suite granitique de Nueltin sont associées à un dyke d'aplite et à un filon pegmatitique. Ces roches sont riches en uranothorite et en allanite, minéraux qui sont également présents dans le granite encaissant de Nueltin. Le dyke d'aplite est enrichi en uranium (56,8 ppm) et en thorium (770 ppm), tandis que le filon pegmatitique est enrichi en uranium (610 ppm), en thorium (8839 ppm) et en terres rares (86 153 ppm au total). Ces concentrations sont de 10 à 100 fois supérieures à celles dans le pluton encaissant. La similarité entre les spectres d'éléments traces de ces roches et ceux du granite encaissant indique que les occurrences anomales représentent fort probablement des liquides magmatiques très fractionnés des phases tardives de cristallisation du granite de Nueltin.

INTRODUCTION

Recent investigations, as part of the Geo-mapping for Energy and Minerals Program (Northern Uranium for Canada Project), assessed the potential of Paleoproterozoic igneous rocks of the Dubawnt Supergroup (Gall et al., 1992) as sources and hosts for uranium deposits. The southernmost extent of the Dubawnt Supergroup is represented by coarse-grained porphyritic granite plutons (Nueltin suite) near Nueltin Lake. The Nueltin Lake granite terrane straddles the Nunavut-Manitoba border and lies within the Southern Hearne Domain of the Western Churchill Province (Fig. 1). The geology is dominated by Archean quartzofeldspathic granitoid rocks (tonalite through granite) with minor septa of supracrustal rocks which form part of the Ennedai belt (Hanmer et al., 2004), overlain by Paleoproterozoic sedimentary rocks of the Hurwitz Group (Aspler et al., 2001). Extensive Paleoproterozoic plutons dated by van Breemen et al. (2005) constitute the Hudson granitoid suite (ca. 1.83 Ga) and the Nueltin granite suite (ca. 1.75 Ga). Inherited zircon geochronology of the Hudson granites and Sm-Nd model ages from both suites indicate that the crust in this part of the Southern Hearne is mainly of ca. 2.7 Ga vintage, but must contain small domains up to 3 Ga old (Peterson et al., 2002).

The Nueltin Lake area is the type location for the Nueltin granite suite. Nueltin plutons are mostly restricted to a 'corridor' (Fig. 1; Peterson et al., 2002) extending mainly from northern Manitoba to south of Schultz Lake, and including outliers in the area of the Amer mylonite zone and Edehon Lake, farther north and east, respectively. The southern end of the Nueltin corridor is interpreted to represent the deepest exposed facies of Nueltin granite, whereas the comagmatic Pitz Formation rhyolite is only found at the northern end of the corridor. Nueltin granite is interpreted to represent highly evolved anorogenic (A-type) granites. Uranium-lead zircon geochronology (van Breemen et al., 2005) indicates all Nueltin plutons were emplaced between 1765 and 1750 Ma, peaking at 1754 Ma. Anorogenic (A-type) granites are commonly enriched in incompatible elements as well as some base metals (such as Cu, Sn, and Pb) and concentrations of Th, U, and Au, due to their highly evolved nature (Gill, 2010).

Mineral occurrences in the Nueltin Lake area were previously described by Charbonneau and Swettenham (1986) as comprising uraninite and uranium-bearing silicate minerals within a tourmaline-bearing granite to quartz monzonite, and locally derived float of sulphide-bearing calc-silicate metasedimentary rocks inferred to predate the Hurwitz Group. Recent field work by the authors, however, has reconfirmed that primary mineral occurrences are hosted by Nueltin granite, suggesting that the Nueltin suite is a potential source of uranium, thorium, and rare-earth elements. This introduces the possibility that the mineral occurrences located within the older adjacent Hudson granite are related to emplacement of the Nueltin granite.

In the Nueltin Lake area (NTS 65 B/4) fieldwork conducted in June 2009 (Table 1) included sampling exposed outcrops of Nueltin granite plutons (Fig. 2). Two anomalous occurrences of radioactivity were discovered using a calibrated RS-230 portable multispectral spectrometer (manufactured by Radiation Solutions Inc.) in survey mode and reported in counts per second (cps). The first occurrence (station 09PHA-J05) is a fine-grained granitic (aplite) dyke. The second occurrence (station 09PHA-J06), located 70 m to the north, is a pegmatitic granite seam within the same pluton.

This paper documents the elevated radioactivity and explores the potential significance of the Nueltin granite suite at Nueltin Lake, as a source of uranium, thorium, and rare-earth elements (REE). Hand samples were cut and studied in detail in via polished thin-section microscopy, scanning electron microscope (SEM), and electron microprobe (EMP) at the Geological Survey of Canada (GSC) in Ottawa. Autoradiographs were taken of polished slabs over an exposure period of four months, except where indicated, also at the GSC. Samples were crushed and pulverized in an agate mill in preparation for whole-rock geochemical analysis by X-ray fluorescence (XRF) at the University of Ottawa, and by inductively coupled plasma mass spectrometery (ICP-MS) at Acme Labs Inc. in Vancouver.

FIELD OBSERVATIONS

Host Nueltin Granite

The host Nueltin granite (Fig. 3), a rapakivi-type granite, consists predominantly of white to pink, weakly aligned, megacrystic potassium feldspar with interstitial coarse plagioclase, smoky quartz, and coarse to very coarse biotite (Fig. 4). The average K-feldspar crystal size is 2 to 3 cm, but up to 5 cm is not uncommon, with a typical length-to-width ratio of 1:2. K-feldspar phenocrysts have coarse perthitic texture and are generally poikilitic, enclosing euhedral biotite and quartz. Plagioclase is commonly saussuritized

Table 1. Location of Nueltin granite samples (in NAD83).

Sample station	Latitude	Longitude
09PHA-J03	60.21025	-99.96575
09PHA-J04	60.21102	-99.96765
09PHA-J05	60.21169	-99.96723
09PHA-J06	60.21222	-99.96789
09PHA-J08	60.20775	-99.96483
09PHA-J10	60.20701	-99.96873
09PHA-J11	60.09195	-100.13496
09PHA-J13	60.09311	-100.13944
09PHA-J14	60.09539	-100.11749
09PHA-J18	60.09036	-100.13814
09PHA-J20	60.18143	-100.12568
09PHA-J21	60.17512	-100.12920
09PHA-J22	60.17068	-100.13015
09PHA-J23	60.16903	-100.13271

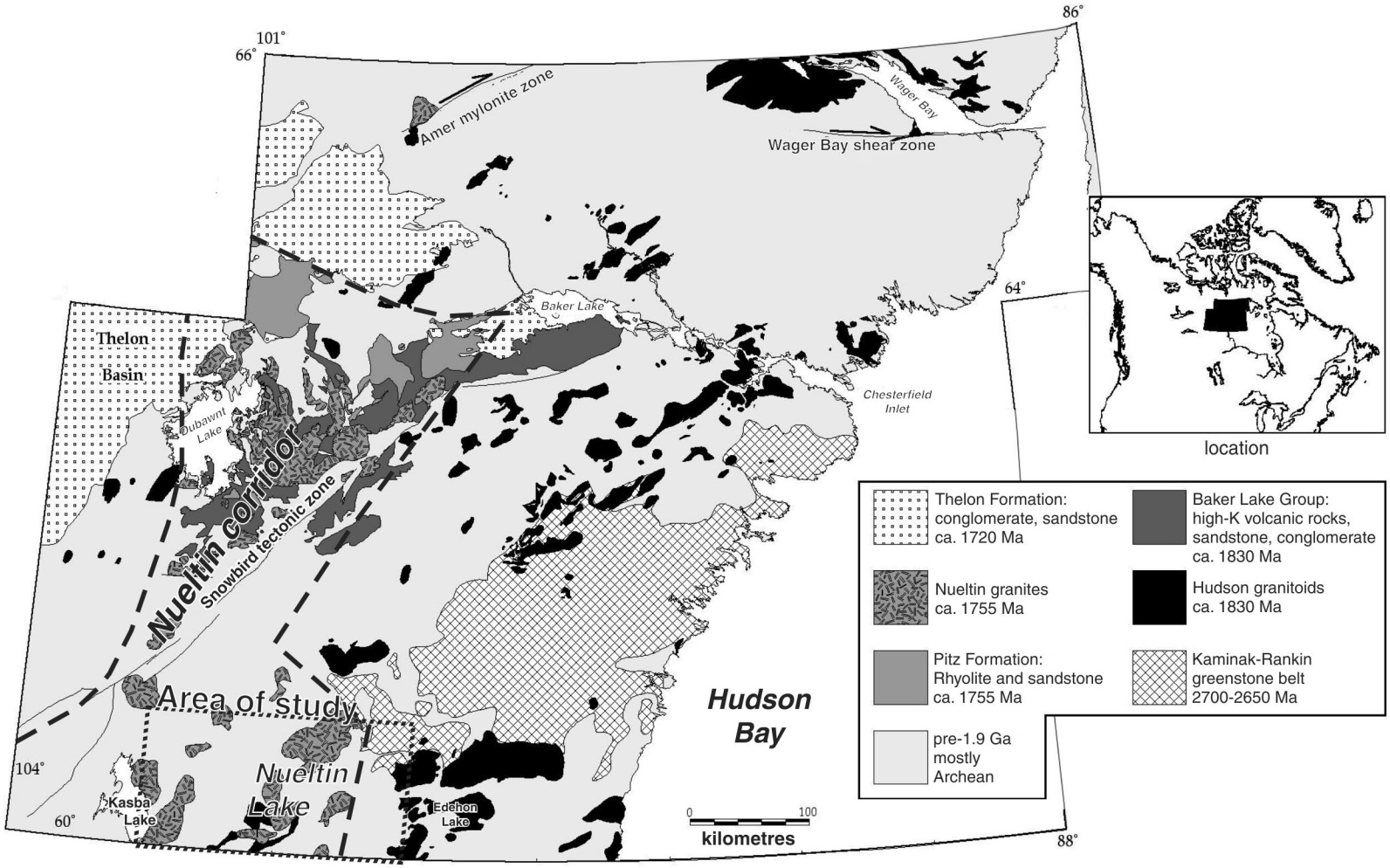

Figure 1. Proterozoic units of the Western Churchill Province (WCP), Nueltin corridor outlined. Area of study at Nueltin Lake highlighted (*modified from* Peterson et al., 2002).

and appears greenish, infrequently occurring as large (up to 3 cm), resorbed sieve-textured phenocrysts with inclusions of biotite and quartz. The Nueltin granite also contains significant accessory fluorite in crystals up to 0.5 cm in diameter. Nueltin outcrops have consistent background radioactivity measured at 200 to 300 cps by gamma-ray spectrometer.

Contacts between the Nueltin plutons and country rock are predominantly sharp. Xenoliths of local Proterozoic sedimentary rocks and Archean basement gneisses are commonly caught up in the marginal phases. The xenoliths are typically angular, rarely greater than 30 cm in length, and generally aligned parallel to the primary igneous alignment of feldspars.

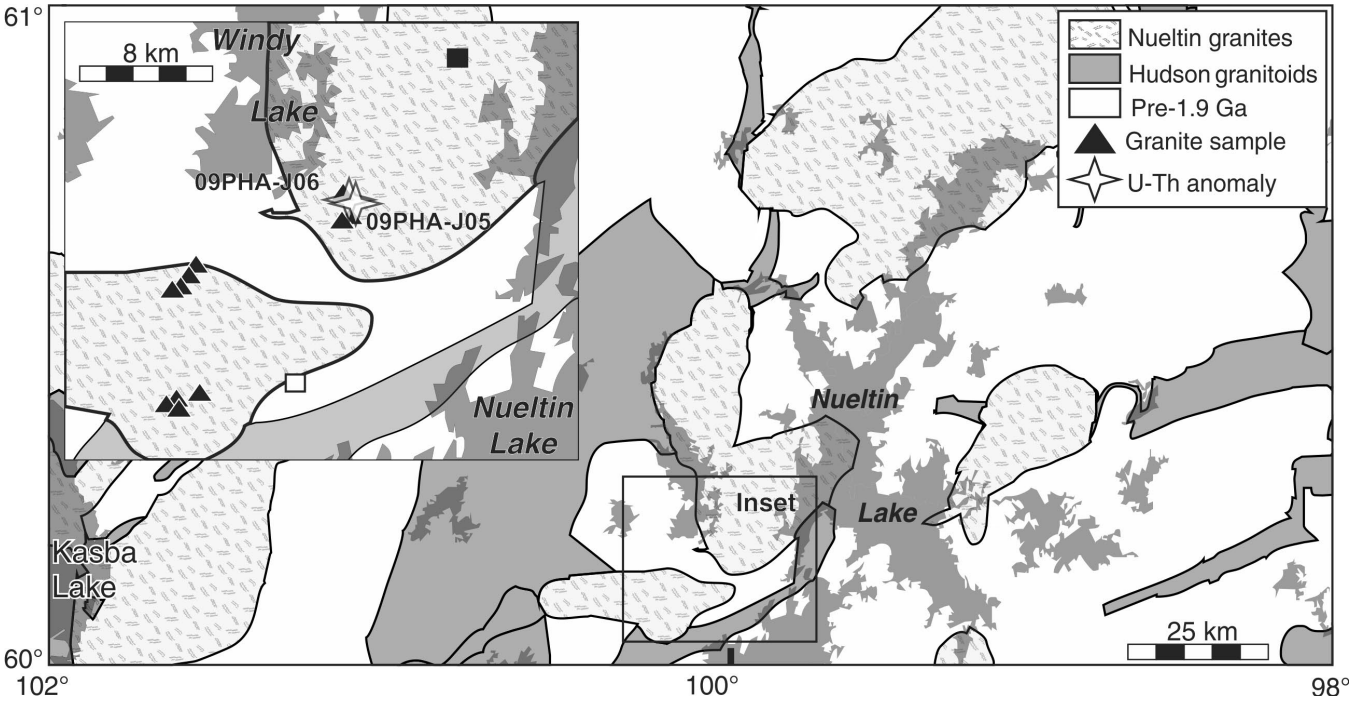

Figure 2. Nueltin Lake study area. Sample locations marked on inset, with anomalous U-Th samples labelled. The filled square (■) indicates a 'vein' occurrence containing Th and REE and the open square (□) represents a polymetallic skarn deposit, both located by Charbonneau and Swettenham (1986).

Figure 3. Outcrop of typical porphyritic Nueltin granite which hosts the samples 09PHA-J05 and 09PHA-J06. Abundant phenocrysts of K-feldspar show weak alignment toward the bottom of the photo. Rock hammer for scale. 2011-189

Figure 4. Polished slab of Nueltin granite showing typical mineralogy and coarse texture. Larger K-feldspar crystals are commonly oikocrystic. At centre, a resorbed plagioclase feldspar with inclusions of quartz and biotite. 2011-190

Bedrock exposures of the anomalously radioactive zones are recessively weathering and are covered by lichen and minor gossanous rubble. This has resulted in a small surface exposure of the pegmatite dyke, requiring the use of a hammer and chisel to obtain three large shards of sample 09PHA-J06.

Fine-grained aplite dyke (sample 09PHA-J05)

The aplite dyke sample is heterogeneous, weakly foliated, and fine to medium grained. The dyke is primarily quartz and K-feldspar, with up to 30% biotite. Fine-grained crystals of purple fluorite are common. Thorite and allanite are significant accessory phases. The thorite typically forms fine-grained (0.1–0.3 mm) anhedral crystals that have weathered to a ruddy brown colour. The allanite is anhedral, has a sub-metallic lustre with greenish hue, and forms random clusters throughout the sample. The heterogeneous, weak foliation in the aplite is defined by biotite and is most evident at transitions between the fine- to medium-grained feldspar and quartz. Contact relationships are obscured by cover but the dyke appears to grade outward from medium- to fine-grained texture. An in situ response of up to 4000 cps was obtained from the gamma-ray spectrometer.

Pegmatitic granitic seam (sample 09PHA-J06)

This sample was taken from a 10 cm wide pegmatitic seam hosted by Nueltin granite. The seam outcrops along a length of approximately 2 feet with a strike of 280°. Contact relationships with host granite were difficult to determine due to lichen cover. The outcrop sample is dominated by coarse K-feldspar, quartz, biotite, allanite, and dark purple fluorite. The seam gave an approximate in situ reading of 9000 cps.

PETROGRAPHY AND MINERALOGY OF OCCURRENCES

Host Nueltin granite

In the host Nueltin granite, K-feldspar phenocrysts consist primarily of microcline-albite perthite. Plagioclase (oligoclase to andesine as determined by EMP), has undergone minor sericitization. Myrmekitic intergrowth between quartz and plagioclase is observed. Iron-rich biotite (annite) is typically spatially associated with zircon and apatite, and these minerals are common as inclusions. Zircon typically occurs as large (100–200 µm), prismatic, euhedral crystals. Dark purple fluorite is associated with biotite. Amphibole (Fe-rich hornblende) is common, though not widespread, as fine-grained, anhedral crystals, showing resorption features and surrounded by quartz (Fig. 5). Titanite is very common as smaller euhedral blades and few larger, subhedral crystals, reaching 0.5 cm. The larger crystals appear mottled in backscatter electron (BSE) images and have inclusions of ilmenite. One particular instance of fracture filling is by allanite with a secondary, plumose REE carbonate mineral (Fig. 6). Allanite typically forms fine-grained (0.4 mm), subhedral crystals, and very fine zoning is visible with cross-polarized light. Autoradiographs of Nueltin granite show that most radioactive minerals are spatially associated with fluorite.

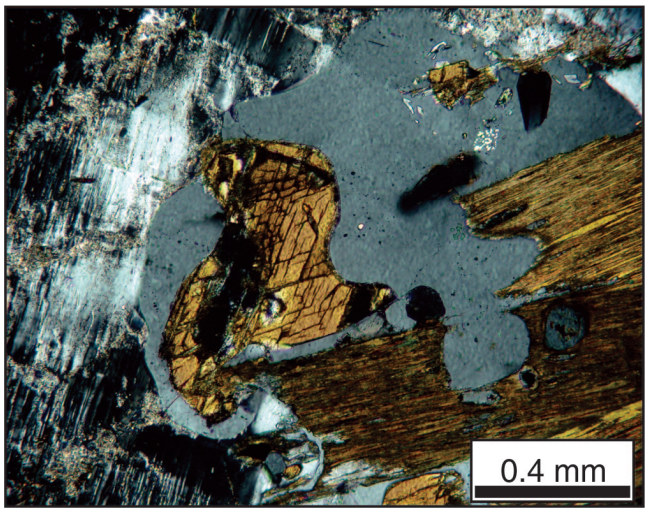

Figure 5. Anhedral hornblende surrounded by a pool of quartz (crossed polars). Adjacent minerals are biotite (lower right) and K-feldspar (left). 2011-192

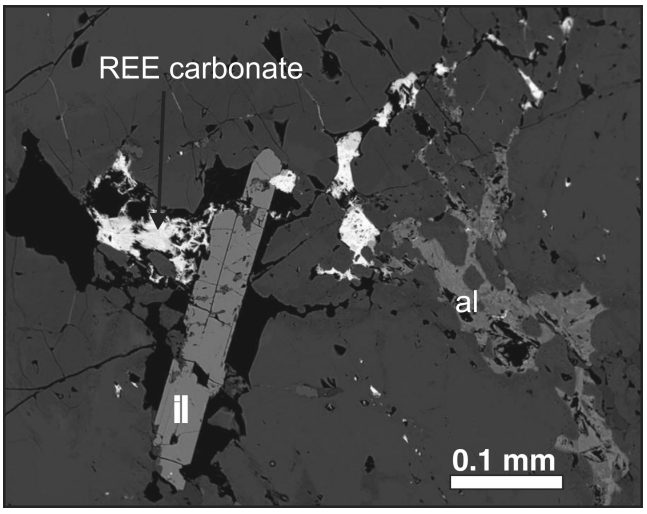

Figure 6. SEM electron backscatter image of detail within a 0.5 cm titanite crystal. The subhedral ilmenite (il) crystal is a primary magmatic inclusion. Fractures are filled by allanite (al) and a secondary REE carbonate mineral. 2011-185

Fine-grained aplite dyke (09PHA-J05)

In thin sections cut from this sample (Fig. 7a), myrmekitic texture between plagioclase and quartz predominates. The composition of feldspar phases (as determined by EMP) in the aplite is identical to that of the host pluton, although some plagioclase is moderately sericitized. The principal source of radioactivity as identified by autoradiograph (Fig. 7b) is thorium, predominantly contained in thorite crystals that are commonly 0.2–0.3 mm in length. The condition of the thorite grains ranges from heavily metamict and altered to relatively unaltered cores of fresh thorite with marginally altered rims. The thorite is spatially associated with apatite, zircon, and biotite.

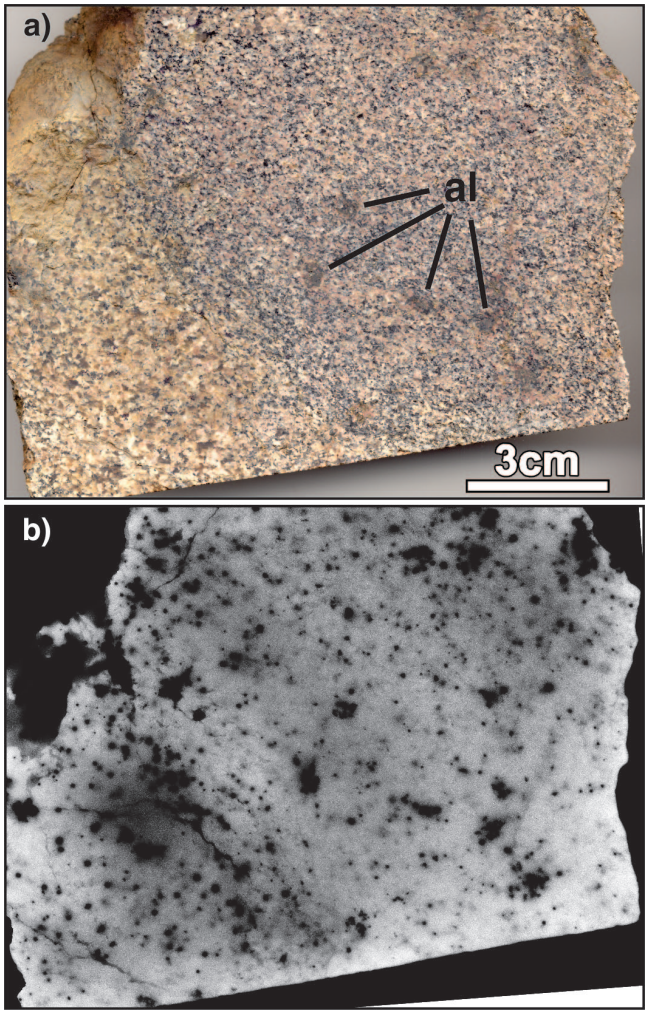

Figure 7. a) Polished slab of aplite sample 09PHA-J05; note fine grain size, heterogeneity, and weak foliation defined by biotite. Large dark grains are allanite (al) with metamict alteration haloes. 2011-186 **b)** Autoradiograph negative of a). Dark areas coincide with allanite (larger) and thorite (smaller) crystals. The distribution of radioactive minerals appears to be unrelated to the foliation. 2011-087

Pegmatitic granitic seam (sample 09PHA-J06)

An autoradiograph (two-week exposure) of the polished slab (Fig. 8a) for this sample showed radioactive allanite crystals (Fig. 8b) up to 3 cm long (average 1 cm) that have a submetallic lustre and greenish colouration. Their preferred orientation perpendicular to the inferred contact is interpreted to be a primary comb texture. Energy-dispersive X-ray spectroscopy (EDS) analysis determined that the primary host minerals of U and Th are subhedral to anhedral, internally heterogeneous uranothorite crystals, which also contain minor quantities of several light rare-earth elements (LREEs): Ce, Nd, and Sm. The SEM imaging and microprobe analysis confirm the REEs are predominantly within subhedral allanite crystals, a few of which are clearly twinned. The allanite crystal rims are depleted

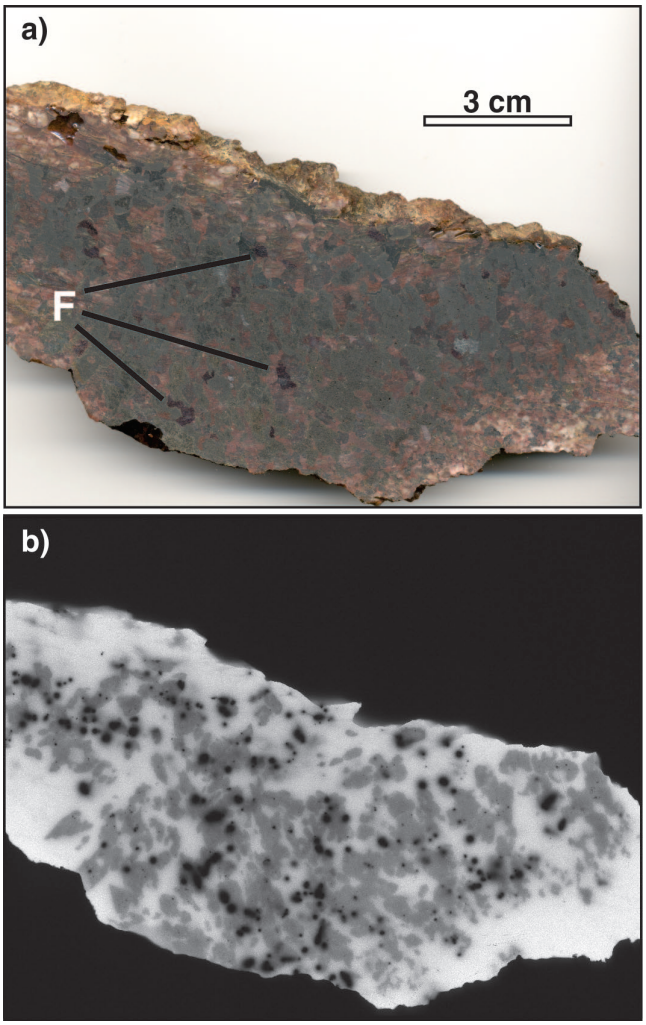

Figure 8. a) Polished slab of 09PHA-J06 showing coarse fluorite (F) and allanite (dark, submetallic). An increased volume due to radiation damage of mineral structures has caused subparallel fracturing along the length of the sample. 2011-191 **b)** Autoradiograph negative of a). Film exposed over two weeks highlights spatial association of radioelement-bearing minerals, allanite (light grey) and uranothorite (black). 2011-194

in LREEs relative to the cores (Fig. 9). The uranothorite and allanite show a very strong spatial association, as the former commonly form inclusions in the latter. Parallel to subparallel fractures transecting the sample are unaffected by mineral boundaries. Radial fractures around uranothorite are related to metamict alteration. Typically, the radial fractures are infilled by a secondary REE carbonate mineral that is also observed, though much less commonly, in the host Nueltin granite (Fig. 10). Allanite was also observed in contact with a symplectic intergrowth of rutile and titanite.

GEOCHEMISTRY

Samples were prepared for XRF analysis of whole-rock major elements at the University of Ottawa by lithium metaborate flux and fusion in a platinum crucible. Total weight was measured before and after to determine volatiles lost on ignition (LOI). The fused samples were analyzed by a Philips PW2400 X-ray fluorescence spectrometer. Trace-element content and metal contents were determined by Acme Labs Inc. using ICP-MS, following a lithium metaborate/tetraborate fusion and nitric acid digestion (package 4B) and aqua regia digestion (package 1DX), respectively. Samples marked with an (*) have values that are an average of duplicated analyses (Table 2). Results were plotted using GDCkit 2.3 (Janoušek et al., 2006).

Host Nueltin granite

The local Nueltin suite granite has slightly lower than typical SiO_2 (weight per cent) and slightly higher CaO, MgO, and Fe_2O_3 (total), compared to other Nueltin granite samples (Peterson et al., 2002; Scott et al., unpub. data, 2011). The local granite is slightly metaluminous, according to the alumina index of Shand (A/CNK versus A/NK (Molecular $[Al_2O_3/(CaO+Na_2O+K_2O)]$ versus $[Al_2O_3/(Na_2O+K_2O)]$)). Relative to bulk continental crust (Fig. 11; Taylor and McLennan, 1995) the host Nueltin Lake granite is generally enriched in large-ion lithophile elements (LILE) and high field-strength elements (HFSE), typical of the Nueltin granite (Peterson et al., 2002). The Th content ranges between 15.5 and 41.25 ppm and the U content between 4.6 and 5.7 ppm, with an average ratio of 5.0 for Th/U (Fig. 12). The host granite is also enriched in total REE (Σ REE 238–413 ppm) and Y (49–66 ppm), and the neighbouring pluton has even higher total REE contents (711–1081 ppm). Chondrite-normalized values (Nakamura, 1974) show slight variations between the local Nueltin plutons, and strong overall enrichment in LREEs (Fig. 13). Apparent REE fractionation within the mineralized granite is less pronounced (LaN/YbN ratio of 4.3–9.5) compared to the other nearby pluton (LaN/YbN = 18.2–44). Additionally, the host Nueltin granite shows a pronounced negative europium anomaly (Eu/Eu* (Eu/Eu* = $Eu_N/[Sm_N*Gd_N]^{0.5}$)) of 0.5, slightly smaller than is typical for the suite.

Fine-grained aplite dyke (sample 09PHA-J05)

The aplite dyke is characterized by a higher silica content (70 wt %), and slightly lower values of CaO and Fe_2O_3 (total), relative to the local granite, and is weakly metaluminous. Overall, the sample has trace-element abundances similar to the host granite (e.g. Fig. 11), with a few exceptions. This sample has notably higher Zr (1062 ppm) and Hf (37 ppm). The anomalously high Th (770 ppm) and U (57 ppm) values (ratio of 13.5) reflect the high modal abundance of thorite.

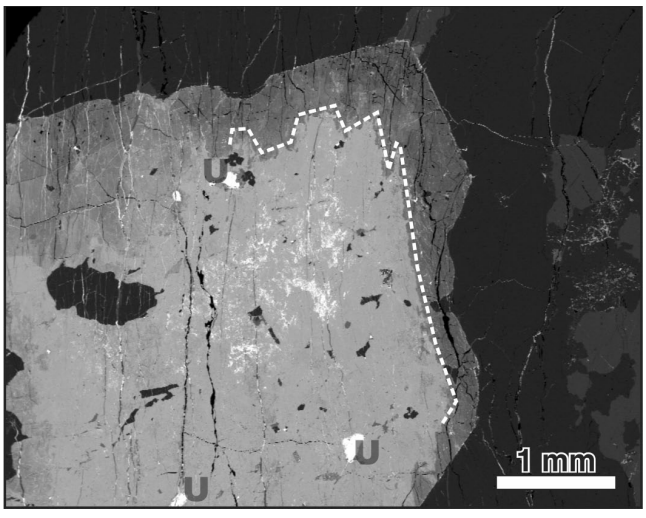

Figure 9. Electron backscatter image of 09PHA-J06 showing large subhedral allanite crystal with contrasting core and rim; reflectivity variation is due to difference in REE content. Bright areas in the core consist of uranothorite (U) and irregular patches of REE metals. 2011-193

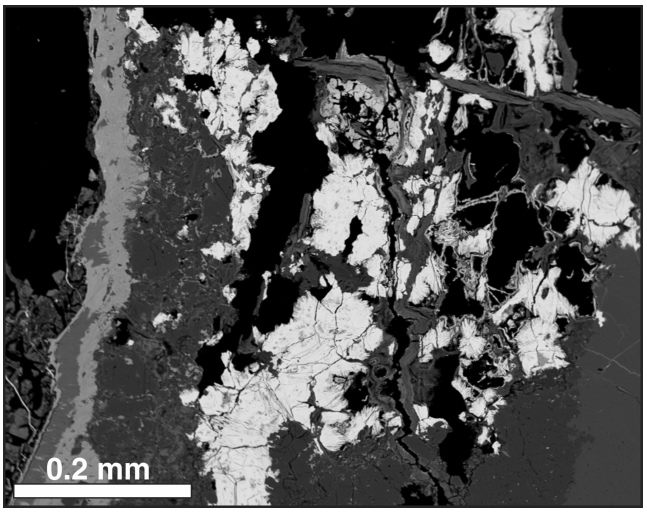

Figure 10. Electron backscatter image of 09PHA-J06 showing acicular and plumose masses of secondary REE carbonate mineral (bright white) adjacent to allanite (lower right). 2011-188

Table 2. Whole-rock elemental analyses of Nueltin granites from Nueltin Lake study area.

Sample	09PHA-J03*	09PHA-J04	09PHA-J08	09PHA-J10*	09PHA-J11	09PHA-J13	09PHA-J14	09PHA-J18*	09PHA-J21	09PHA-J22	09PHA-J23*	09PHA-J05*	09PHA-J06*
Intrusion	Nueltin granite	Nueltin granite	Nueltin granite	Nueltin granite	Nueltin granite	Nueltin granite	Nueltin granite	Nueltin granite	Nueltin granite	Nueltin granite	Nueltin granite	Aplite dyke	Pegmatitic seam
SiO_2	66.44	67.1	67.38	65.87	69.57	71.83	68.93	70.2	71.77	67.84	72.4	70.005	47.92
Al_2O_3	14.39	13.55	13.92	14.52	13.3	12.75	14.10	13.41	12.81	13.93	12.245	13.595	11.60
CaO	2.44	2.40	2.39	2.45	1.22	1.21	1.49	1.28	1.11	1.62	1.39	1.54	5.89
K_2O	5.16	4.66	5.16	5.26	6.03	5.85	6.10	6.552	6.05	5.82	5.00	5.99	2.44
MgO	0.51	0.64	0.52	0.58	0.26	0.32	0.37	0.3	0.36	0.38	0.31	0.325	0.79
MnO	0.07	0.09	0.07	0.07	0.03	0.04	0.04	0.03	0.03	0.05	0.03	0.04	0.12
Na_2O	3.00	2.78	2.79	2.94	2.43	2.24	2.57	2.38	2.2	2.74	2.55	2.89	0.52
P_2O_5	0.19	0.23	0.19	0.26	0.14	0.14	0.20	0.15	0.14	0.18	0.11	0.16	0.01
Fe_2O_3total	4.93	6.25	4.52	5.20	3.17	3.47	3.92	3.36	3.52	4.89	3.64	2.79	9.19
TiO_2	0.61	0.72	0.56	0.67	0.32	0.36	0.46	0.37	0.35	0.50	0.37	0.36	0.78
Cs	7.6	11.9	10.2	4.15	5.5	6.7	6.9	6.1	6.8	9.6	6.8	5.7	3.7
Ga	25.9	26.2	24.4	24	25	24	26.3	23.6	23.8	27.6	23.2	20	34.6
Hf	12.6	13.8	11.9	12.9	11.1	10.6	13.7	11.9	11.9	16.6	13.6	37.8	3.4
Nb	33.4	40.6	36.4	29.4	30.5	30.1	36.1	26.9	29.8	39.8	26.7	17.3	17.3
Rb	315.45	345.4	337.5	261.5	381.3	381.7	393.9	377.8	379.2	423.3	317.75	315.0	119.8
Sr	229.6	208.6	233.7	249.7	100.6	95.4	104.4	110.7	86.8	112.4	121.7	184.0	493.6
Ta	1.7	2.1	3.4	1.9	1.4	1.7	1.9	1.4	1.6	1.8	1.5	0.8	1.9
Th	20.9	15.5	23.4	41.3	126.2	109.5	116.7	189.7	123.6	100.6	99.6	769.9	8838.8
U	5.2	5.3	5.7	4.6	6.5	9.2	6.4	6.05	4.7	6.3	11.75	57.2	610.3
Zr	446.4	512.6	409.1	467.8	338.6	352	451.6	352.6	361.5	541.3	441.2	1062.3	79.3
Y	51.8	56.2	66.2	49.6	37.5	43	42	50.3	39	65.5	51.7	42.3	843.4
La	40.5	36.3	45.0	72.2	189.7	172.8	204.8	238.2	195.8	157.0	242.2	110.7	22494.6
Ce	85.7	84.9	100.9	172.4	396.7	377	444.6	490.3	412.3	324.2	531.6	174.5	45119.9
Pr	11.95	12.22	15.70	23.54	42.88	41.21	48.96	50.88	45.04	35.97	55.43	17.92	4287.36
Nd	54.1	55.7	65.8	91.5	147.0	143.8	172.9	173.8	156.5	128.7	185.3	63.4	11559[a]
Sm	11.24	12.13	13.27	15.44	20.26	20.77	25.33	21.96	21.24	19.85	24.36	9.21	1428.13
Eu	1.8	1.7	1.9	2.20	1.25	1.19	1.36	1.31	1.06	1.29	1.33	1.38	36.72
Gd	10.00	10.42	11.02	11.60	11.9	12.97	16.64	13.77	13.1	14.76	14.94	7.66	701.67
Tb	1.61	1.67	1.92	1.74	1.54	1.84	2.12	1.88	1.61	2.30	2.16	1.21	68.48
Dy	8.98	9.01	10.97	9.24	6.79	8.19	8.64	9.03	6.84	11.55	10.60	6.71	257.68
Ho	1.76	1.8	2.19	1.76	1.18	1.43	1.39	1.61	1.09	2.14	1.86	1.40	32.38
Er	5.11	5.26	6.68	5.02	3.16	3.72	3.46	4.36	2.8	6.18	5.19	4.28	75.05
Tm	0.79	0.83	1.03	0.77	0.44	0.56	0.52	0.65	0.41	0.93	0.76	0.66	10.76
Yb	5.14	5.58	6.82	5.07	2.88	3.49	3.55	4.24	2.80	5.77	4.73	4.55	72.03
Lu	0.76	0.88	1.05	0.76	0.42	0.51	0.51	0.6	0.44	0.83	0.69	0.76	10.18
Pb	13.3	13.9	10.2	17.85	23.9	18.9	21.9	30.1	14.4	28.8	17.7	107.0	957.8
F	3032	3230	3470	2414	2190	2360	2730	3008	2520	3560	3392	3045	9740

All major elements were analyzed by XRF and trace elements by ICP (see text).
* Indicates the values for the sample are a calculated average from duplicated analyses.
[a] Indicates Nd value determined by XRF only.

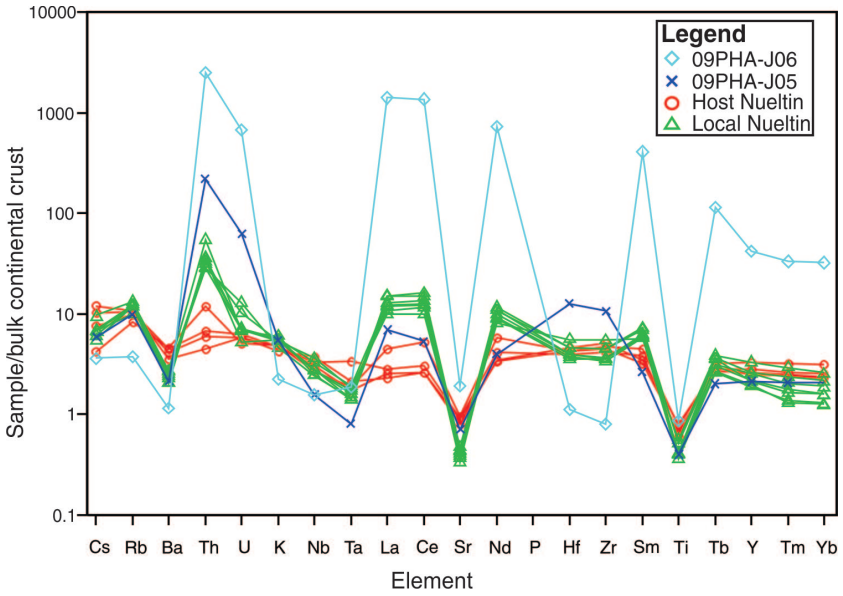

Figure 11. Nueltin granite compositions normalized to continental crust (after Taylor and McLennan, 1995). The element patterns of the granite samples are parallel to sub-parallel, consistent with a simple genetic relationship by crystal fractionation.

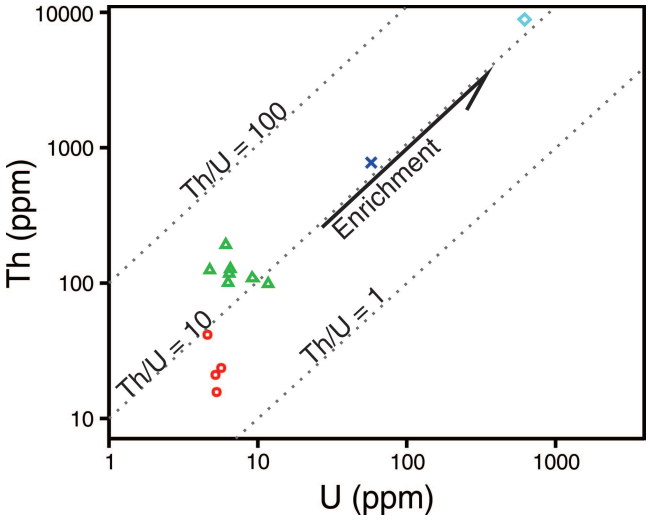

Figure 12. Log - log plot of Th versus U for selected Nueltin granites. The observed constancy of Th/U supports magmatic fractionation as the cause of enrichment for 09PHA-J05 and 09PHA-J06. Symbols are the same as in Figure 11.

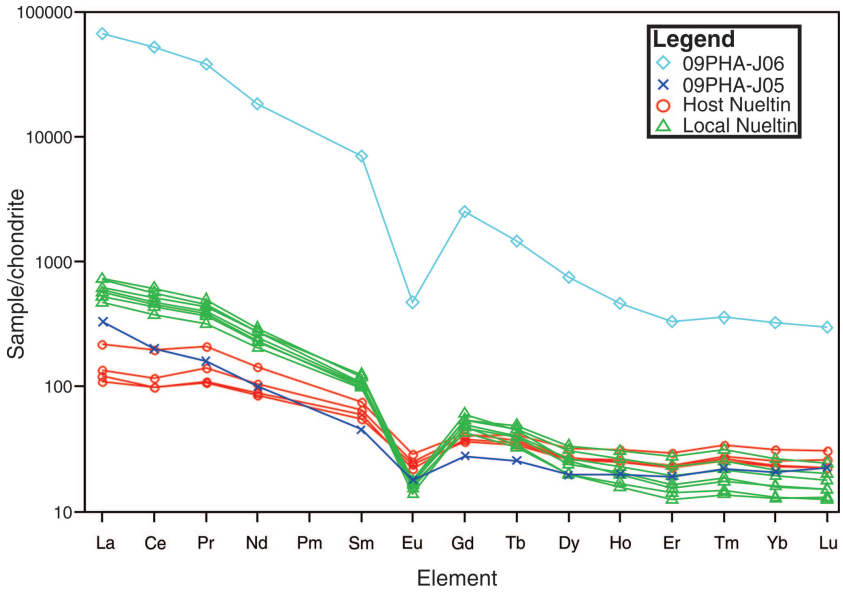

Figure 13. REE compositions normalized to chondrites (*after* Nakamura, 1974).

Rare-earth element trends correlate with the host Nueltin granite, total LREEs (366 ppm) and HREEs (10 ppm), but have a slightly higher La_N/Yb_N ratio of 16.3. The negative Eu anomaly (0.5) is similar to that of the host Nueltin pluton. Base metal concentrations, i.e. W, Zn, Cu, Mo, and Ni, are also low relative to those of the host.

Pegmatitic granitic seam (sample 09PHA-J06)

In comparison to the host Nueltin granite, the seam has much lower SiO_2 (<50 wt %) and Na_2O (CaO/Na_2O = 10). Conversely, CaO and Fe_2O_3 (total) are higher. The sample is strongly metaluminous. The trace-element chemical signature of this sample parallels that of Nueltin granite in general, but some element enrichments or depletions are more pronounced. The most pronounced depletions, relative to the host granite, are those of phosphorus (80 ppm), Zr (79 ppm) and Hf (3 ppm). Pronounced enrichments, relative to the host, are in Th (8838 ppm) and U (610 ppm), giving a Th/U ratio of 14.4, compared to the average Nueltin granite Th/U ratio of 11.9 (Fig. 12). This sample is strongly enriched in REEs, as exemplified by Figure 13, with a concentration of approximately Σ REEs 84 500 ppm (Σ LREEs = 83 460 ppm; Σ HREEs = 168 ppm) and La_N/Yb_N ratio of 208. The strong negative europium anomaly (approximately 0.1) is more pronounced than that of the host granite. Also, F constitutes nearly 1% of the analyzed sample. Relative to the average local granite, the seam is low in W, Cu, Mo, and Ni, with much higher contents of As, Cd, and Bi.

INTERPRETATION AND SUMMARY

The mineralogy of both the dyke and seam resemble the mineralogy of the host granite and other local Nueltin plutons. Additionally, geochemical trends are consistent with a cogenetic relationship between the host granite and both 09PHA-J05 and 09PHA-J06. The aplite dyke (09PHA-J05) is likely a chilled, late-stage melt segregated from the host Nueltin granite. It is geochemically very similar to the host granite; the relatively high radioelement, Zr, and Hf contents represent strong fractionation of high field-strength elements. The biotite foliation may reflect magmatic flow as the fracture hosting the melt widened. The pegmatitic seam (09PHA-J06) is also interpreted as a late-crystallizing partition that records extreme fractionation, but its unusual major-element composition is unlikely to represent an actual magma, therefore the pegmatite may have crystallized from percolating intergranular melts. The seam is strongly enriched in all REEs but shows significant fractionation between LREE relative to HREE. Enrichment by magmatic fractionation is also supported by the co-variation of Th and U from the unfractionated to more fractionated samples.

Charbonneau and Swettenham (1986) discovered a less enriched 'vein' (Th = 460 ppm, REE = 0.2%) in the same Nueltin pluton 12.5 km to the northeast (Fig. 2), which may represent a related occurrence. It is probable that minor, highly enriched bodies of this type are widely dispersed in these coarse, fractionated granite plutons. The high concentrations of U, Th, and REE, and the metamict nature of the allanite and thorite would facilitate mobilization and subsequent anomalous concentrations of radioactive elements within organic materials and possibly as secondary precipitates. Lake sediment geochemistry data by McCurdy et al. (in press) show that previously mapped Nueltin granite plutons in the Nueltin Lake area correspond closely to areas of strong positive anomalies in LREEs (Ce, La, Nb) and Y in the lake sediments (Fig. 14). One large anomaly shown on the east side of Figure 14 is not associated with any mapped granitic body, indicating that additional unmapped Nueltin bodies may be present. Lake sediment geochemistry is proposed as a useful means of predicting as yet unmapped outcrops of Nueltin granite within the Edehon Lake area and possibly regionally within the greater Western Churchill Province.

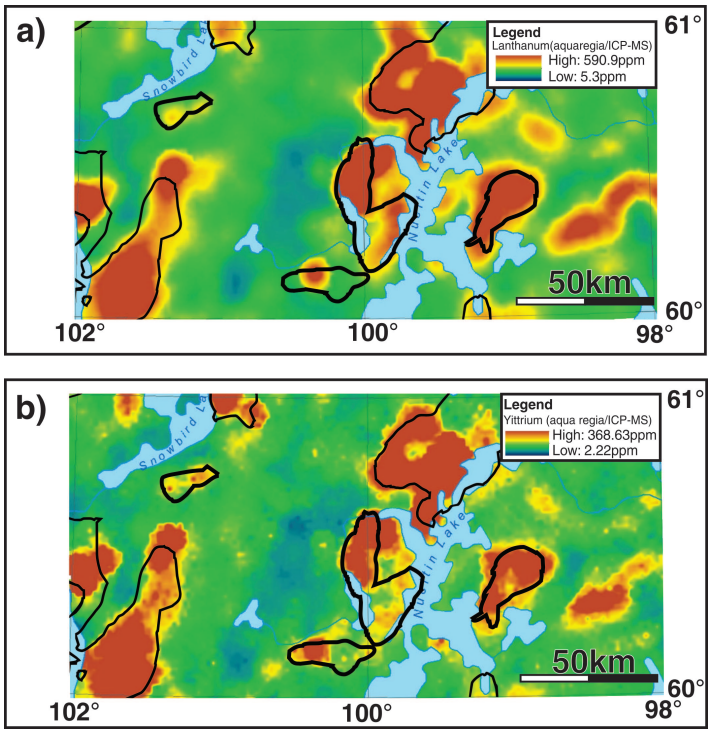

Figure 14. Map of lake-sediment analyses (McCurdy et al., in press) of **a)** La and **b)** Y. High concentrations of La and Y correlate strongly with the extents of known Nueltin plutons (black outlines; *from* Paul et al., 2002).

ACKNOWLEDGMENTS

This study is part of a M.Sc. thesis supported through the Research Affiliate Program by the Geo-mapping for Energy and Minerals Program delivered by the Geological Survey of Canada, in Ottawa. The authors would like to thank Katherine Venance for microprobe work and Pat Hunt for her work on the SEM and assistance with developing of autoradiograph film. Reviews and suggestions from Bruce Kjarsgaard, Brian Cousens, and Charlie Jefferson greatly improved the paper. Cameco Corporation generously provided access and logistical support. Re-evaluation of lake sediment surveys was instigated by Sally Pehrsson. This study is part of the Northern Uranium for Canada Project aimed at improving the understanding of uranium deposits located within and around the Thelon Basin, in particular the roles that Paleoproterozoic granite suites may have played as sources and/or hosts of mineralization.

REFERENCES

Aspler, L.B., Chiarenzelli, J.R., Cousens, B.L., McNicoll, V.J., and Davis, W.J., 2001. Paleoproterozoic intracratonic basin processes, from breakup of Kenoran to assembly of Laurentia: Hurwitz Basin, Nunavut, Canada; Sedimentary Geology, v. 141–142, p. 287–318. doi:10.1016/S0037-0738(01)00080-X

Charbonneau, B.W. and Swettenham, S.S., 1986. Gold occurrence in radioactive calc-silicate float at Sandybeach Lake, Nueltin Lake area, District of Keewatin; *in* Current Research 1986-A; Geological Survey of Canada, p. 803–808.

Gall, Q., Peterson, T.D., and Donaldson, J.A., 1992. A proposed revision of Early Proterozoic stratigraphy of the Thelon and Baker Lake basins, Northwest Territories; *in* Current Research, Part C; Geological Survey of Canada, Paper 92–1 C, p. 129–137.

Gill, R., 2010. Igneous Rocks and Processes: A Practical Guide, Wiley-Blackwell, 440 p.

Hanmer, S., Sandeman, H.A., Davis, W.J., Aspler, L.B., Rainbird, R.H., Ryan, J.J., Relf, C., Roest, W.R., and Peterson, T.D., 2004. Neoarchean tectonic setting of the Central Hearne supracrustal belt, western Churchill Province, Nunavut, Canada; Precambrian Research, v. 134, p. 63–83. doi:10.1016/j.precamres.2004.04.005

Janoušek, V., Farrow, C.M., and Erban, V., 2006. Interpretation of whole-rock geochemical data in igneous geochemistry: introducing Geochemical Data Toolkit (GCDkit); Journal of Petrology, v. 47, p. 1255–1259. doi:10.1093/petrology/egl013

McCurdy, M.W., McNeil, R.J., Pehrsson, S.J., and Day, S.J.A., in press. Regional lake sediment and water geochemical data, Nueltin Lake Area, Nunavut (NTS 65A, 65B and 65C) Geological Survey of Canada, Open File 6986, 1 CD-ROM. doi:10.4095/289888

Nakamura, N., 1974. Determination of REE, Ba, Fe, Mg, Na and K in carbonaceous and ordinary chondrites; Geochimica et Cosmochimica Acta, v. 38, p. 757–775. doi:10.1016/0016-7037(74)90149-5

Paul, D., Hanmer, S., Tella, S., Peterson, T.D., and LeCheminant, A.N., 2002. Compilation, bedrock geology of part of the western Churchill Province, Nunavut – Northwest Territories Geological Survey of Canada, Open File 4236, 2002; 1 sheet 1 CD-ROM, doi:10.4095/213530

Peterson, T.D., Van Breemen, O., Sandeman, H., and Cousens, B., 2002. Proterozoic (1.85–1.75Ga) igneous suites of the Western Churchill Province: granitoid and ultrapotassic magmatism in a reworked Archean hinterland; Precambrian Research, v. 119, p. 73–100. doi:10.1016/S0301-9268(02)00118-3

Taylor, S.T. and McLennan, S.M., 1995. The geochemical evolution of the continental crust; Reviews of Geophysics, v. 33, p. 241–265. doi:10.1029/95RG00262

van Breemen, O., Peterson, T.D., and Sandeman, H.A., 2005. U-Pb zircon geochronology and Nd isotope geochemistry of Proterozoic granitoids in the western Churchill Province: intrusive age pattern and Archean source domains; Canadian Journal of Earth Sciences, v. 42, p. 339–377. doi:10.1139/e05-007

Geological Survey of Canada Project EGM007